104 (2025) 105058

Contents lists available at ScienceDirect

Poultry Science

journal homepage: www.elsevier.com/locate/psj

Identification of key genes associated with residual feed intake in small-sized meat ducks through integrated analysis of mRNA and miRNA transcriptomes

Dandan Geng [a,b], Chunyou Yuan [b], Xiaofan Li [a,b], Chenxiao Wang [a,b], Qixin Guo [b], Yong Jiang [b], Zhixiu Wang [b], Guohong Chen [a,b], Guobin Chang [a,b], Hao Bai [a,*]

[a] Joint International Research Laboratory of Agriculture and Agri-Product Safety, the Ministry of Education of China, Institutes of Agricultural Science and Technology Development, Yangzhou University, Yangzhou 225009, PR China
[b] Key Laboratory of Animal Genetics and Breeding and Molecular Design of Jiangsu Province, Yangzhou University, Yangzhou 225009, PR China

ARTICLE INFO

Keywords:
Residual feed intake
small-sized meat ducks
hypothalamus
miRNA–mRNA network
miR-182-5p

ABSTRACT

As a major producer and consumer of duck meat, China faces industry challenges due to low feed conversion efficiency. Residual feed intake (**RFI**), a key metric for poultry feed utilization, remains poorly characterized in small-sized meat ducks. We raised 1,000 ducklings with similar initial body weight (**BW**) under controlled conditions until 63 days of age. RFI was calculated using average daily gain (**ADG**), average daily feed intake (**ADFI**), and metabolic body weight ($\mathbf{MBW^{0.75}}$). Thirty high-RFI (**HRFI**) and thirty low-RFI (**LRFI**) ducks were selected to evaluate growth performance. Hypothalamic samples from 6 HRFI and 6 LRFI ducks underwent transcriptomic analysis, including differential gene expression, gene ontology, Kyoto Encyclopedia of Genes and Genomes pathway analysis, weighted gene co-expression network analysis, and miRNA target prediction. Results showed that the LRFI group had significantly lower feed intake (**FI**) and ADFI than the HRFI group ($P < 0.05$). Compared to low RFI controls, HRFI meat ducks exhibited 45 differentially expressed (**DE**) miRNAs (6 upregulated and 39 downregulated) and 323 DE mRNAs (133 upregulated and 190 downregulated), enriched in substance and energy metabolism pathways. Weighted gene co-expression network analysis identified ten hub DE miRNAs, including miR-1-3p, miR-10-5p/3p, miR-182-5p/3p, miR-183-5p, miR-263-5p, miR-96-5p, miR-7, and novel-m0108-5p. miRNA–mRNA network analysis revealed 43 DE regulatory pairs, including 15 with negative feedback. Notably, miR-182 targeted and regulated the highest number of DE mRNAs, showing negative feedback interactions with *DDC, UPP2, PRSS35*, and *SLCO1C1*. Dual-luciferase reporter assays confirmed the binding of partial genes. Given *DDC*'s role in dopamine and serotonin synthesis, we further validated the miR-182-5p/*DDC* regulatory relationship through overexpression, interference, and Western blot experiments. This study provides novel insights into the molecular mechanisms underlying feed efficiency in ducks.

Introduction

China plays a significant role in the global duck meat farming industry as a prominent producer and consumer of duck meat. According to data from the China Animal Husbandry Association and the Food and Agriculture Organization of the United Nations, China produced 4.218 billion commercial meat ducks in 2023, representing approximately 70% of global production for that year. Rising consumer expectations and an emphasis on product quality have led to a heightened demand for premium, small-sized meat ducks. However, the industry faces challenges, such as slow growth rates and low feed efficiency. Current breeding programs aimed at improving feed intake (**FI**) are progressing slowly, prompting a shift toward enhancing feed utilization efficiency in farm animal production. Feed conversion ratio (**FCR**) is crucial for assessing the efficiency of feed utilization in livestock and poultry (Cantalapiedra-Hijar et al., 2018). This ratio is negatively correlated with pivotal economic indicators including body weights (**BWs**) and daily weight gain (Crews, 2005). Genetic selection targeting the optimization of FCR can indirectly enhance the physical dimensions and conformation of livestock and poultry as well as augment muscle fiber

* Corresponding author.
E-mail address: bhowen1027@yzu.edu.cn (H. Bai).

https://doi.org/10.1016/j.psj.2025.105058
Received 2 December 2024; Accepted 16 March 2025
Available online 21 March 2025

diameter, ultimately influencing meat quality (Listrat et al., 2016). Therefore, the FCR is inadequate for the selection of high-quality, small-sized meat ducks. Residual FI (**RFI**) denotes the discrepancy between the actual and anticipated FI necessary for the maintenance and growth of animals (Koch et al., 1963). Notably, choosing ducks with a low-RFI can boost FI without impairing production performance (Bai et al., 2022a). Concurrently, RFI can enable the identification of ducks that exhibit lower feed consumption rates and accelerated growth patterns (Li et al., 2023). Additionally, research has linked intestinal flora to RFI in small-sized meat ducks, revealing that the microbiota involved in carbohydrate metabolism can positively affect FI (Bai et al., 2022b). Currently, research on small-sized meat ducks is primarily focused on production, with relatively little research on their genetic regulation and molecular mechanisms.

FI in livestock and poultry is largely influenced by the hypothalamus (Tran et al., 2016). The hypothalamus plays a crucial role in modulating feed conversion efficiency by regulating foraging behavior and the expression of relevant genes. The hypothalamic–pituitary–adrenal (**HPA**) axis, recognized for its involvement in stress responses and feeding behavior regulation, releases corticotropin-releasing hormone, adrenocorticotropic hormone (**ACTH**), and glucocorticoids (**GCs**), which subsequently influence RFI (Mokshata and Tanmay, 2021). In meat ducks, notable alterations in hypothalamic mRNA concentrations may be associated with RFI (Zeng et al., 2016). MicroRNAs (**miRNAs**) are vital endogenous small non-coding RNAs that regulate gene expression and are crucial in controlling feed intake and energy metabolism. For example, 10 miRNAs have been identified in cattle that are potentially implicated in modulating biological pathways pertinent to RFI (De Oliveira et al., 2018). In poultry, investigations have revealed a noteworthy correlation between the A95T upstream miRNA-1596 mutation and RFI trait (Luo et al., 2015). However, the roles of miRNAs in targeting specific mRNA that regulate feed efficiency in duck meat have not been extensively studied. This study aimed to address the research gap by examining the microRNA-mediated regulation of hypothalamic feed efficiency and energy metabolism in meat ducks, offering novel insights into improving feed utilization efficiency in this species.

Transcriptomics involves the study of gene function and structure and often employs high-throughput sequencing techniques. In systems biology, the weighted gene co-expression network analysis (**WGCNA**) is a widely adopted method that uses multiple samples to explore biological inquiries (Devis et al., 2020; Núria et al., 2022; Yang et al., 2019). By integrating high-throughput sequencing technology with WGCNA, researchers can identify key genes strongly associated with specific traits. This process entails clustering genes exhibiting similar expression patterns into modules and investigating the biological correlations between these co-expression modules and target traits. In this study, high-throughput sequencing and WGCNA were employed to identify crucial mRNA–miRNA regulatory network linked to RFI traits in small-sized meat ducks. The study aimed to establish a molecular framework for understanding the regulatory mechanisms of RFI in small-sized meat ducks by comparing changes in gene expression levels between high- and low-RFI meat ducks.

Materials and methods

Ethics Statement

All experimental procedures, including animal handling, were performed in strict adherence to the experimental protocol approved by the Animal Care and Use Committee of Yangzhou University (Protocol No. SYDW-2019015). All experimental procedures were carried out by trained personnel who minimized handling time and employed gentle restraint techniques to reduce stress. Prior to the experiment, the ducks were acclimated to their new environment to mitigate stress associated with environmental changes. All interventions were performed in accordance with animal welfare regulations.

Animal Preparation and Experimental Design

A total of 1,200 1-day-old small-sized meat ducks (H2 strain with black beak, black shank, and white feathers), comprising equal numbers of males and females, were sourced from the Ecolovo Group (ShuYang, China) in China. In the first two weeks, all ducks were housed on the floor at a density of 15 ducks per square meter. At 14 d of age, 1,000 ducks of similar weight were chosen and placed in separate cages of 73 × 55 × 80 cm (about 1 m^2 each). Each cage was furnished with feeders and drinkers. The experimental period spanned 21–63 d, during which all ducks were provided unrestricted access to food and water.

Growth Performance Measurement

The entire experiment spanned 42 d, with the initial BW (**iBW**) recorded on day 22 and the final BW (**fBW**) assessed on day 63. We measured the growth performance of 30 ducks, such as metabolic BW (**$MBW^{0.75}$**), body weight gain (**BWG**), average daily gain (**ADG**), feed intake (**FI**), average daily feed intake (**ADFI**), and FCR, were derived from data gathered between days 22 and 63. $MBW^{0.75}$ was computed as fBW increased to 0.75. RFI was determined using the methodology outlined by Aggrey et al. (2010) through the subsequent equation:

$$\mathrm{RFI} = \mathrm{ADFI} - \left(a + b_1 \times \mathrm{MBW}^{0.75} + b_2 \times \mathrm{ADG}\right),$$

where a denotes the intercept, b_1 represents the regression coefficient of FI relative to $MBW^{0.75}$, and b_2 represents the regression coefficient of FI concerning ADG.

Sample Collection

At 63 days of age, 12 healthy meat ducks with similar BWs were selected from four groups: low-RFI male duck group (**LRM**), low-RFI female duck group (**LRF**), high-RFI male duck group (**HRM**), and high-RFI male duck group (**HRF**). Each group was replicated three times to minimize experimental errors. After anesthesia with CO_2, the selected ducks were promptly euthanized by exsanguination through the carotid artery. The entire brain was extracted and transferred to a clean sampling table. Hypothalamic tissue specimens were obtained and rapidly snap-frozen in liquid nitrogen prior to storage at –80°C for subsequent RNA extraction and sequencing.

Isolation of Total RNA and Construction of RNA-Seq Libraries

Total RNA was isolated with TRIzol reagent (Invitrogen, Hong Kong, China). Subsequently, the integrity of RNA was analyzed with an Agilent 2100 Bioanalyzer (Agilent, CA, USA), and meanwhile, RNA purity was evaluated based on the OD260/280 and OD260/230 ratios using NanoPhotometer spectroscopy (IMPLEN, USA). RNA concentrations were quantified with a Qubit 2.0 Fluorometer (Life Technologies, CA, USA). All RNA samples exhibited optical density (260/280) values > 1.8 and RNA integrity number values > 8.0, indicating suitability for library construction and deep sequencing. Following library preparation, mRNA and miRNA sequencing was conducted utilizing the Illumina NovaSeq platform (Illumina NovaSeq 6000). Standard quality control measures were applied to the downstream RNA data using FASTP (Chen et al., 2018) to filter low-quality and invalid data. Sequencing alignment files were generated by aligning clean reads to the reference genome of ducks (GCA_017639305.1) using HISAT2 software (version 2.2.1) for statistical and analytical assessment of RNA expression. Detailed information onregarding the mapping results is presented in supplementary Table S2. After initial filtering of the small RNA data, sequences lacking a 3′ linker, containing a 5′ linker, or with a polyA tail were also excluded. miRNAs were identified by selecting small RNA sequences derived from annotation sequencing of rRNA, scRNAs, snoRNAs, snRNAs, and tRNA from the GenBank and Rfam databases. The miRNA identification results

are presented in supplementary Table S1.

Statistical and Bioinformatics Analysis

Differential expression analysis was employed to identify differentially expressed (**DE**) miRNAs and mRNAs in the hypothalamus of meat ducks with high and low RFI. RNA-seq count data analysis of brain tissue samples was conducted utilizing DESeq2 (version 1.16.1) software. To ensure accurate analysis of gene differences, we used FPKM values to estimate mRNA expression levels and TPM values to estimate miRNA expression levels. The screening criteria for differentiating DE miRNAs and mRNAs were set as $|\log2FC| \geq 1$, and the threshold of significance was $P \leq 0.05$. DIANA Tools-mirPath was used for the functional annotation of DE miRNAs. DAVID online software (https://david.ncifcrf.gov/) was used for DE mRNA Gene Ontology (**GO**) analysis and Kyoto Encyclopedia of Genes and Genomes (**KEGG**) gene and genome function enrichment analysis. Additionally, miRNA–mRNA pairs were identified through predicted miRNA–mRNA interactions using TargetScan, TarBase, and Miranda (v3.3a). The resulting miRNA–mRNA pairs were utilized to establish a miRNA–mRNA interaction network. The study's workflow is illustrated in Fig. 1.

Construction of miRNA WGCNA and Identification of Significant Modules

We employed the WGCNA package in R to discover gene co-expression network modules linked to RFI traits in meat ducks. To assure network accuracy, we initially screened and filtered the gene set to exclude low-quality genes or samples that could bias the results, retaining genes with a median absolute deviation greater than 0.01. Hierarchical clustering using the hclust function in WGCNA helped identify and remove outliers from the miRNA data samples. We used the Pearson correlation coefficient to establish a co-expression similarity matrix to evaluate gene pair correlations. The soft threshold β was determined using the R function pickSoftThreshold guided by the scale-free topology requirement. In this study, the optimal soft threshold power β value was set to 5 ($R^2 > 0.8$), and the topological matrix was constructed accordingly. Cluster analysis of the topological matrix identified nine modules, with a minimum module size of 30 miRNAs and modules with correlation coefficients exceeding 0.75. Subsequently, each module was subjected to correlation analysis to assess its relevance. Module significance (**MS**) was used to measure the correlation strength, with the module exhibiting the highest MS score designated as the key module. Genes within these key modules were identified as candidate core miRNAs influencing RFI traits in meat ducks.

Cell Culture and Plasmid Transfection

The duck embryo fibroblast cell line (**DEF**) was obtained from Wuhan Pricella Biotechnology Co., Ltd. (Wuhan, China) and cultivated in high-glucose Dulbecco's modified Eagle's medium (BasalMedia, Shanghai, China) supplemented with 10% fetal bovine serum. The incubator conditions were set at 37°C with 5% CO_2 concentration. The miR-182-5p mimic, NC mimic, miR-182-5p inhibitor, and NC inhibitor were purchased from GenePharma (Shanghai, China) and transfected utilizing the Lipofectamine 3000 reagent (Invitrogen, Carlsbad, CA, USA).

Total RNA Isolation and Real-time Quantitative Polymerase Chain Reaction (RT-qPCR)

RNA was extracted from duck hypothalamic tissue samples and DEF using TRIzol reagent (Invitrogen, USA). The total RNA was then reverse transcribed into cDNA for mRNA analysis using the FastKing gDNA Dispelling RT SuperMix kit (TIANGEN, China), whereas miRNA was transcribed using the miRcute Plus miRNA First-Strand cDNA Synthesis Kit (TIANGEN, China). RT-qPCR was conducted utilizing the PowerUp™ SYBR™ Green Master Mix kit (ABI, USA) under the following conditions: 95°C for 10 min, 40 cycles of 95°C for 15 s, and 60°C for 1 min, with GAPDH and U6 serving as the internal controls for mRNA and miRNA quantification, respectively. Each reaction included three technical replicates, and expression levels were determined using the $2^{-\Delta\Delta Ct}$ formula (Livak et al., 2001). mRNA primer sequences were designed using the NCBI Primer-BLAST tool (https://www.ncbi.nlm.nih.gov/tools/primer-blast/), and mature miRNA sequences retrieved from the miRBase database (http://www.mirbase.org/) were imported into miRprimer software to design miRNA primers under optimized conditions.

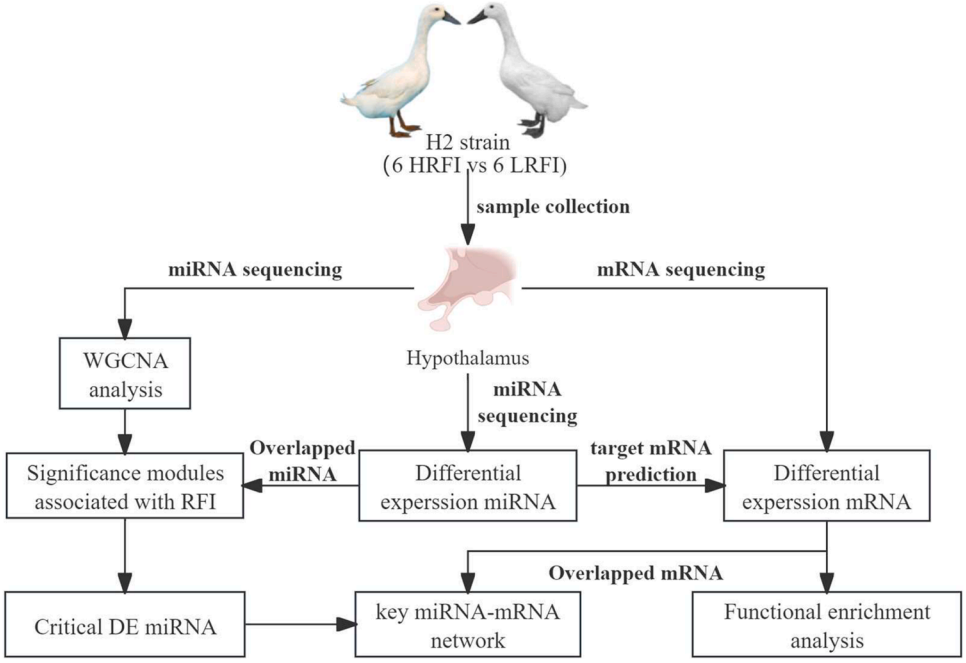

Fig 1. Examine the workflow of the study. Procedure for establishing the miRNA-mRNA regulation network in the hypothalamus of small-sized meat ducks exhibiting varying RFI; RFI refers to residual feed intake; miRNA denotes microRNA; mRNA signifies messenger RNA; PPI indicates Protein-Protein Interaction.

The primer sequences are listed in supplementary Table S3.

Luciferase Reporter Assay

To validate the specific binding between the candidate miRNA and the 3'-UTR of the target gene, we performed a dual-luciferase reporter assay. The wild-type 3'-UTR sequences (WT) of the target gene containing predicted binding sites and their corresponding mutant sequences (MUT) were cloned into the pMIR-REPORT luciferase reporter vector (Thermo Fisher, Shanghai, China). The aforementioned sequences were obtained via PCR amplification using the primers listed in supplementary Table S4. Subsequently, the pMIR-REPORT luciferase reporter vector was co-transfected with either the miR-182-5p mimic or the NC mimic into DEF for 48 hours utilizing the Lipofectamine 3000 transfection reagent (Invitrogen, Carlsbad, California, USA). The cells were ultimately collected, and luciferase activity was evaluated with a dual-luciferase reporter gene assay kit (Beyotime, Shanghai, China).

Western Blot Analysis

Protein samples were collected from DEF cells and their concentrations were evaluated using a BCA Protein Assay Kit (TIANGEN, Beijing, China). The study utilized the following primary antibodies: DDC Rabbit pAb (A3828, 1:500 dilution; ABClonal) and β-Actin Rabbit mAb (AC038, 1:10,000 dilution; ABClonal).

Statistical Analysis

This study utilized SPSS 30.0 software (IBM Corporation, NY, USA) and GraphPad Prism 9.0 (GraphPad Software Inc., CA, USA) for data analysis. A two-tailed Student's t-test was utilized in SAS (version 9.4) to assess significant differences between the two groups for normally distributed data. Values of $P < 0.05$ were deemed statistically significant.

Results

Growth Performance

Table 1 illustrates the impact of RFI divergence on the growth performance of small-sized meat ducks. The findings revealed that FI and ADFI were approximately one-third lower in ducks from the low RFI (**LRFI**) group (6,039.133 g and 143.789 g, respectively) than in those from the high RFI (**HRFI**) group (9,052.633 g and 215.539 g, respectively) ($P < 0.01$). Furthermore, there were highly significant variations in the FCR and RFI between the LRFI (4.102 g and –40.888 g, respectively) and HRFI (6.295 g and 31.928 g, respectively) groups ($P < 0.01$). Notably, significant differences in BW, fBW, $MBW^{0.75}$, BWG, or ADG were not identified between the two groups ($P > 0.05$).

DE miRNAs and mRNAs in Small-sized Meat Ducks with Different RFI

Through small RNA sequencing of 12 hypothalamic tissue samples from both high- and low-RFI ducks, we obtained 11,813,281–18,144,858 clean small RNA reads. Of these, 97.19–98.50% were identified as miRNAs, and the detailed identification results are provided in Table S1. In the comparison between the LR and HR groups, 45 DE mature miRNAs were identified, of which 39 were downregulated and 6 were upregulated, as shown in Fig. 2A. Transcriptome analysis yielded 41,842,074–61,660,290 clean RNA sequences after removing low-quality reads, with 91.75–92.54% successfully mapped to the duck genome (mapping details in Table S2). Additionally, 323 DE mRNAs were identified in the low- and high-RFI groups, with 190 exhibiting downregulation and 133 exhibiting upregulation (Fig. 2B). Heat maps were generated to visualize the expression patterns of the DE miRNAs and mRNAs in ducks with high and low RFI (Fig.s 2C and 2D, respectively). The complete lists of DE miRNAs and mRNAs with annotation details are provided in supplementary Tables S5 and S6, respectively.

Prediction and Visualization of miRNA–mRNA Relationships

The functions of the 45 DE miRNAs ($|\log2FC| \geq 1$ and $P \leq 0.05$) identified in the hypothalamus of high- and low-RFI ducks were annotated using DIANA-mirPath. Thirteen metabolically related KEGG pathways ($P < 0.01$), including metabolic pathways ($P = 2.19E\text{-}06$), PI3K-Akt signaling pathway ($P < 0.05$), and mTOR signaling pathway ($P < 0.01$), were associated with the mRNA targets of these 45 miRNAs (Fig. 3A, B). Additionally, DAVID was utilized for functional annotation of the 323 DE mRNAs ($|\log2FC| \geq 1$ and $P \leq 0.05$) identified in the hypothalamus. GO enrichment analysis revealed several enriched cellular components (**CCs**) among the 323 DE mRNAs, including membranes (GO:0016020), cells (GO:0005623), and organelles (GO:0005575). The molecular functions (**MFs**) included binding (GO:0005488), catalytic activity (GO:0003824), and transporter activity (GO:0005215). In terms of biological processes (**BPs**), enrichment was primarily observed in metabolic processes (GO:0008152), biological regulation processes (GO:0065007), and stimulus-response processes (GO:0050896), which are primarily associated with metabolic regulation and organismal responses (Fig. 3C). KEGG analysis revealed significant enrichment of the DE mRNAs in pathways related to substance or energy metabolism and signaling, such as "protein digestion and absorption," "tyrosine metabolism," "relaxin signaling pathway," "phenylalanine metabolism," "IL-17 signaling pathway," "adipokine signaling pathway," "PI3K-Akt signaling pathway," and "dopaminergic

Table 1
Effects of RFI divergence on the growth performance of small-sized meat ducks from 22 to 63 days of age.

Trait[1]	LRFI			HRFI			SEM	P-value
	LRM	LRF	Mean	HRM	HRF	Mean		
Initial BW (g)	613.333	620	616.667	621.667	646.667	634.167	23.163	0.724
Final BW (g)	2092.333	2083.667	2088	1955	2197.667	2076.333	40.162	0.893
MBW0.75(g)	309.294	308.336	308.815	293.993	320.861	307.427	4.448	0.885
BWG(g)	1479	1463.667	1471.333	1333.333	1551	1442.167	28.858	0.636
ADG (g/d)	35.214	34.849	35.032	31.746	36.929	34.337	0.687	0.636
FI(g)	6034.133	6044.133	6039.133[b]	8692.8	9412.467	9052.633[a]	479.713	<0.001
ADFI (g/d)	143.67	143.908	143.789 [b]	206.971	224.106	215.539 [a]	11.421	<0.001
FCR (g/g)	4.077	4.128	4.102 [b]	6.524	6.066	6.295 [a]	0.342	<0.001
RFI (g/d)	-41.353	-40.423	-40.888 [b]	32.067	31.79	31.928 [a]	11.132	<0.001

[a,b] Within a row for each factor, different superscripts indicate significant differences ($P < 0.05$).

LRFI = low residue feed intake; HRFI = high residue feed intake; SEM = standard error of mean; LRM = low-RFI male duck group; LRF = low-RFI female duck group; HRM = High-RFI male duck group; HRF = High-RFI female duck group; Initial BW = body weight on d 22; final BW = body weight on d 63; $MBW^{0.75}$ = metabolic body weight on d 63; BWG = body weight gain; ADG = average daily gain; FI = feed intake; ADFI = average daily feed intake; FCR = feed conversion ratio; RFI = residual feed intake.

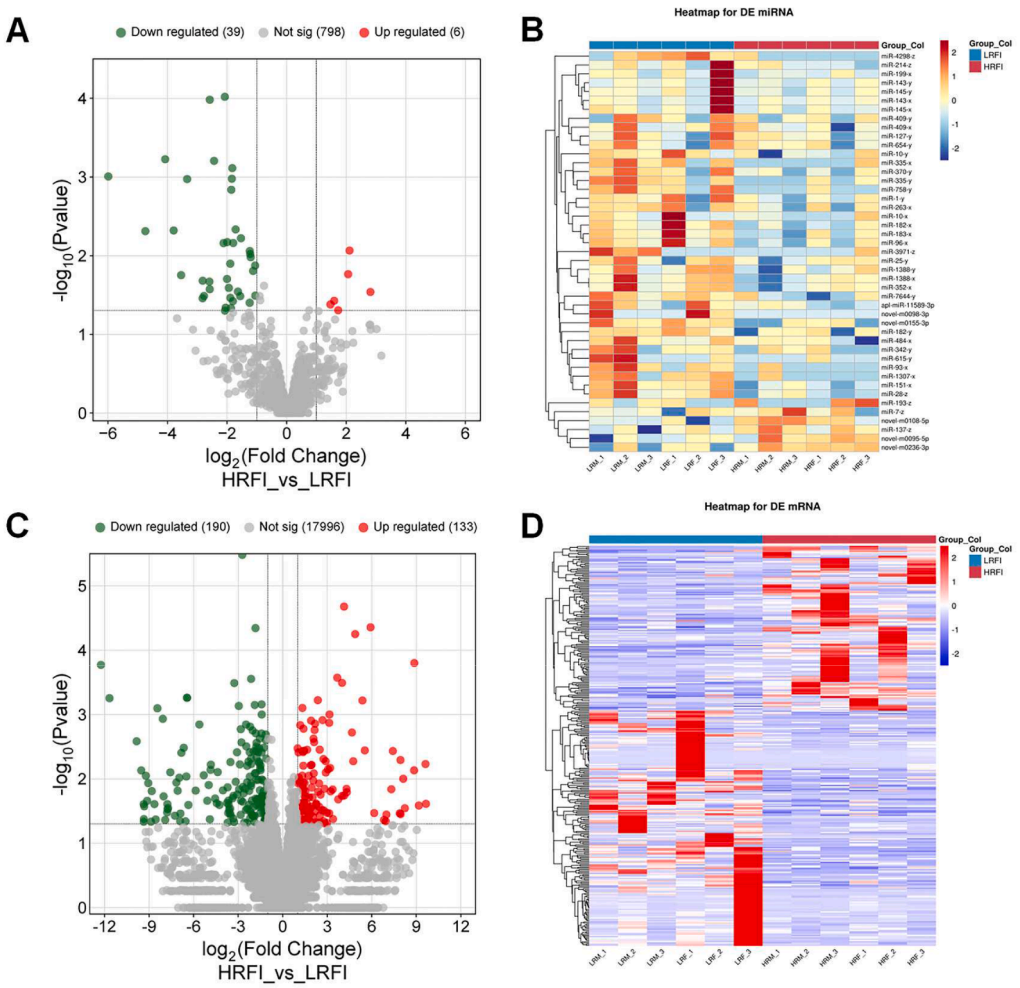

Fig 2. Analysis of DE miRNAs and mRNAs between LRFI and HRFI ducks. A, Volcano plot analysis of DE miRNAs between LRFI and HRFI ducks. B, Heatmap analysis of DE miRNAs between LRFI and HRFI ducks. C, Volcano plot analysis of DE mRNAs between LRFI and HRFI ducks. D, Heatmap analysis of DE mRNAs between LRFI and HRFI ducks.

synapse" (Fig. 3D). These findings suggest a correlation between FI and hypothalamic brain metabolism, signaling, and neural activity.

Construction of Co-expression Network of miRNA

To identify hub miRNAs, we employed the WGCNA method, which is a commonly used approach for identifying co-expressed gene modules, to cluster miRNAs that were highly correlated with RFI traits. The soft threshold was set to 5 in the WGCNA to ensure a scale-free topology (Fig. 4A). After merging highly similar modules, a dynamic tree-cutting algorithm identified nine distinct modules with sizes ranging from 38–147 genes (Fig.s 4B, C). The "gray" module contained unexpressed genes and was excluded from further analysis. We then calculated the correlations between each module and various RFI phenotypic traits. The results revealed that the characteristic genes of the green module (HRM: $R^2 = 0.61$, $P = 0.06$) were strongly associated with HRM, whereas those of the yellow module (LRF: $R^2 = 0.6$, $P = 0.06$) were closely linked to LRF (Fig. 4D). Further analysis of gene–trait correlations within the modules showed that genes in the green module were highly positively correlated with HRM (cor = 0.51, $P = 1.4E{-}06$, Fig. 4E), while genes in the yellow module were strongly positively correlated with LRF (cor = 0.54, $P = 2.3E{-}07$, Fig. 4F). This indicates that the genes in these modules may play key roles in influencing RFI traits. Therefore, genes from these two modules were selected for subsequent functional and mechanistic analyses.

RFI-Related miRNA–mRNA Regulatory Network in the Hypothalamus

By integrating DE miRNAs with genes from the yellow and green modules, we identified 10 DE hub miRNAs that were highly correlated with RFI phenotypes (Fig. 5A). We then predicted the target genes of these 10 miRNAs and compared them with the DE mRNAs. The analysis revealed 43 potential miRNA–mRNA pairs, 15 of which were selected based on the principle that miRNAs negatively regulate mRNA expression (Fig. 5B). These negatively regulated miRNA–mRNA pairs are believed to be critical for the hypothalamic regulation of RFI in ducks. In the present study, the *DDC* gene was primarily enriched in pathways related to tyrosine metabolism, phenylalanine metabolism, and dopaminergic synapses, suggesting their involvement in the regulation of feeding in meat ducks.

Validation of Differential Genes

To validate the findings of the RNA-Seq analysis, we selected five mRNAs (*C7, DDC, PRSS35, LUM*, and *MEOX2*) and five miRNAs (miR-182-5p, miR-183-5p, miR-199-5p, miR-7-5p, and miR-96-5p) that demonstrated significant differences in expression levels. We validated the selected mRNAs and miRNAs via qRT-PCR. Fig. 6 provides visual evidence of the strong agreement between the expression levels obtained from RNA-Seq analysis and qRT-PCR validation. This validation strengthened the reliability of our RNA-Seq findings and supported the

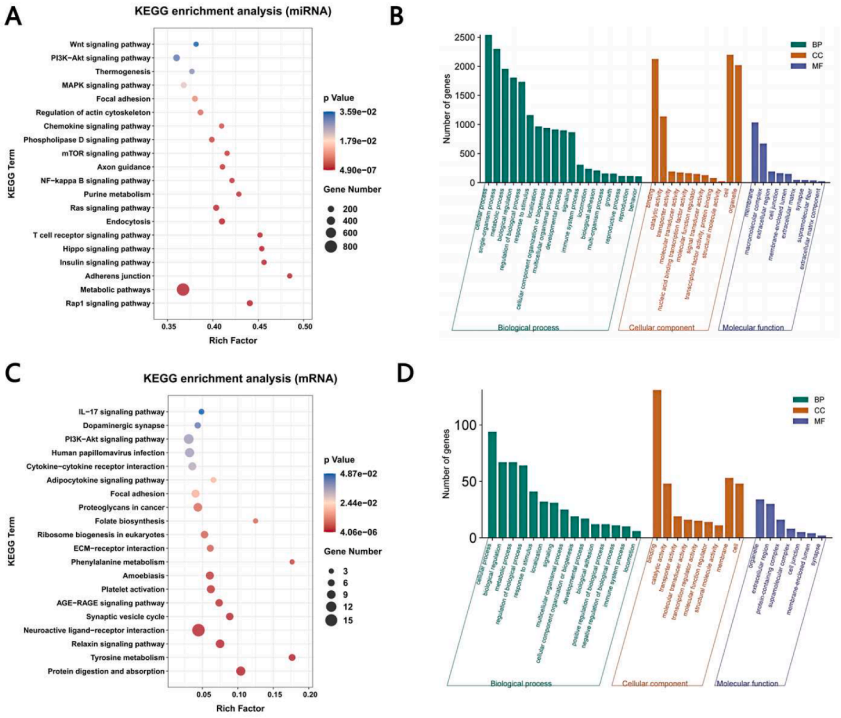

Fig 3. Pathway enrichment analysis of DE genes between LRFI and HRFI ducks. A and B, KEGG and GO enrichment analysis of DE miRNAs between LRFI and HRFI ducks. C and D, KEGG and GO enrichment analysis of DE mRNAs between LRFI and HRFI ducks.

robustness of our gene expression data.

In Vitro Functional Validation of miRNA-mRNA Regulatory Network

To validate the accuracy of the constructed miRNA-mRNA interactions, we selected miR-182-5p as the target miRNA and performed dual-luciferase reporter assays on three predicted target genes. The results demonstrated that compared with the NC mimic, the miR-182-5p mimic significantly suppressed the luciferase activity of wild-type (WT) constructs, while showing no inhibitory effect on their corresponding mutant (MUT) constructs (Fig. 7A-C). These findings confirm that miR-182-5p specifically binds to the 3′UTR regions of Dopa Decarboxylase (***DDC***), Serine Protease 35 (***PRSS35***), and Solute Carrier Organic Anion Transporter Family Member 1C1 (***SLCO1C1***). Notably, given *DDC*'s crucial role in dopamine synthesis (a key neurotransmitter regulating feeding behavior), we further investigated miR-182-5p's regulatory effect on *DDC* using qRT-PCR and Western blot analyses. The experimental data revealed that the miR-182-5p mimic significantly downregulated both mRNA and protein expression levels of DDC, whereas the miR-182-5p inhibitor exhibited opposing effects (Fig. 7D, E).

Discussion

RFI is increasingly acknowledged as a pivotal parameter for evaluating feed efficiency in the livestock and poultry industries (Zhang et al., 2017). Studies have shown that selecting animals with low RFI can enhance feed efficiency in small-sized meat ducks without adversely affecting their production performance (Bai et al., 2022a). This has prompted researchers to delve into the mechanisms underlying RFI to uncover strategies for improving feed efficiency in livestock and poultry. However, most RFI-related studies have concentrated on structural variations and gene expression analyses, with less emphasis on exploring molecular regulatory mechanisms. For example, whole-genome resequencing has been used to identify genomic variations linked to RFI in local and commercial chickens (Liu et al., 2018), and transcriptome analysis of the duodenum has highlighted the correlation between intestinal health-related pathways and RFI in broilers (Liu et al., 2019). Furthermore, transcriptome analysis has highlighted significant miRNA–mRNA network in pig skeletal muscle that correlate with RFI in pigs (Jing et al., 2015). Given the current limited understanding of the miRNA–mRNA network associated with RFI in small-sized meat ducks, the construction of such a network may yield novel insights into the molecular mechanisms governing RFI, potentially facilitating the creation of innovative strategies for enhancing feed efficiency in livestock and poultry.

The hypothalamus is pivotal in the regulation of FI, and a substantial body of research has underscored its role in modulating feeding behavior in livestock and poultry (Yousefvand and Hamidi, 2022). Studies have demonstrated a correlation between hypothalamic gene expression profiles and RFI variations in Nellore bulls (Mota et al., 2017). Notably, Aderibigbe (2022) revealed that dietary phosphorus deficiency reduces feed intake in broilers through modified expression of anorexigenic genes in both intestinal and hypothalamic tissues. Consequently, systematic investigation of gene expression patterns and molecular regulatory mechanisms within the hypothalamic tissue is essential for elucidating the biological pathways governing RFI in poultry species. Emerging evidence has established miRNAs as pivotal regulators in poultry production performance through their multifaceted roles in modulating muscle development (Yuan et al., 2024), lipid homeostasis (Zhai et al., 2023), and endocrine functions (Nouchi et al., 2023), ultimately impacting growth and feed efficiency. Our experimental findings identified 45 DE miRNAs, with their corresponding target mRNAs demonstrating statistically significant enrichment ($P<0.05$) in multiple KEGG pathways, particularly in metabolic pathway, PI3K-Akt signaling pathway, actin cytoskeleton reorganization, insulin signaling pathway, and mTOR signaling pathway. Notably, metabolic pathways exhibited the highest degree of target gene enrichment. Previous studies have revealed that enhancement of the PI3K-Akt signaling pathway and mTOR signaling pathway can effectively improve feed conversion efficiency in practical aquaculture (Zhang et al., 2024), while hypothalamic mTOR/PI3K/Akt signaling

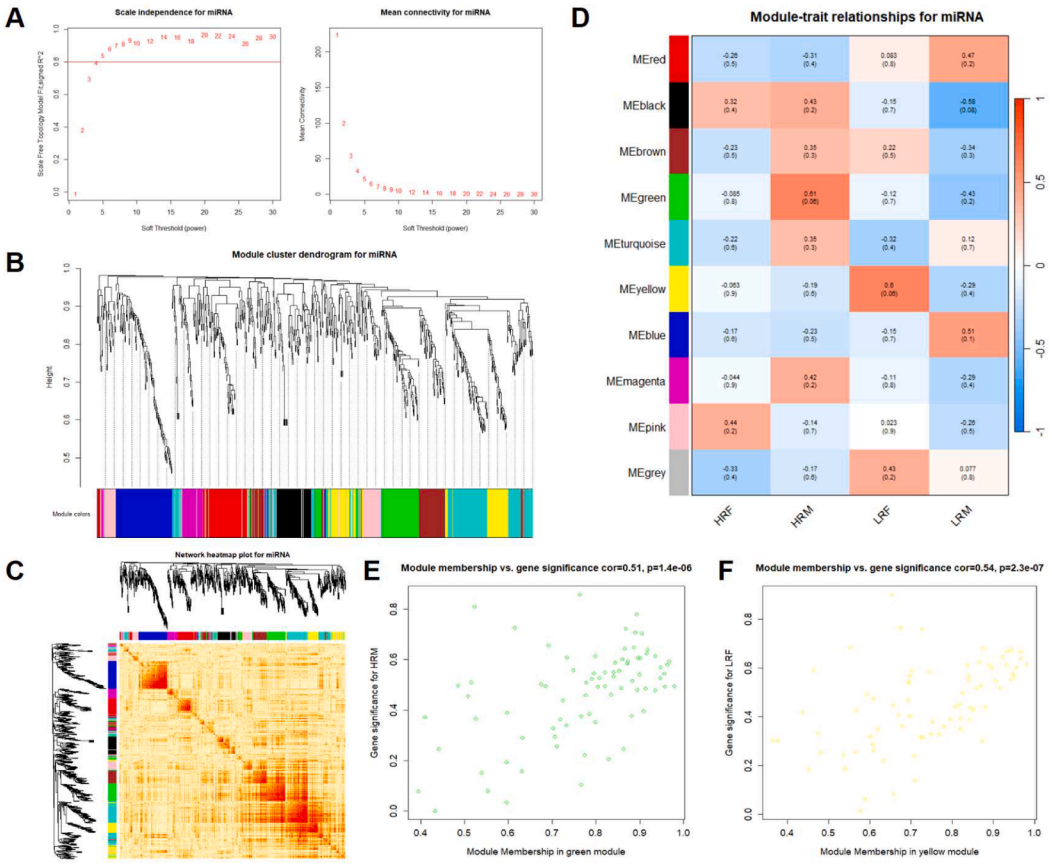

Fig 4. WGCNA analysis. A, Analysis of the fitting index of the scale-free topology model with soft threshold (β) and its mean connectivity. B, Dendrogram illustrating gene clustering according to topological overlap, accompanied with designated module colors. C, TOM map depicting the interrelations among genes. Light colors signify minimal overlap, while dark colors denote significant overlap. Darker color blocks on the diagonal signify co-expression modules. D, Correlation diagram between modules and the risk model. Each cell includes the respective correlation coefficient and *P*-value. E, Scatter plot illustrating the significance of the correlation between the green module and genes inside the HRM. F, Scatter plot illustrating the significance of the relationship between the yellow module and genes inside the LRF.

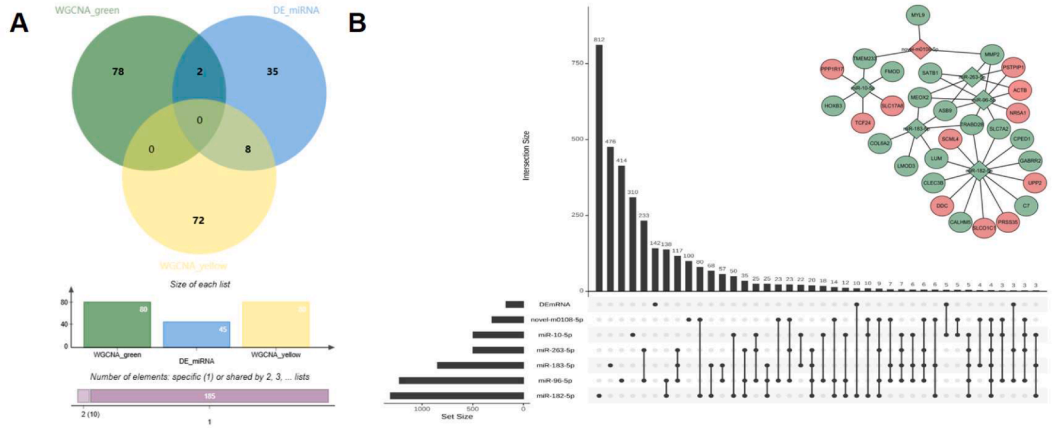

Fig 5. Identification of RFI-associated hub miRNAs and construction of the critical miRNA–mRNA regulatory network. A, Venny diagram of DE miRNAs and genes from key modules of WGCNA. B, Advanced Venny diagram of six key DE miRNAs targeting regulatory genes overlapping with DE mRNAs, along with the miRNA–mRNA regulatory network. Diamonds represent miRNAs; ellipses represent mRNAs. Red indicates upregulated miRNAs or targets, while green indicates downregulated miRNAs or targets.

activation promotes systemic glucose homeostasis through central regulatory mechanisms (He et al., 2021). Transcriptomic investigations comparing high- and low-RFI meat duck pectoralis muscle tissue have established associations between actin cytoskeleton regulation and RFI variation (Wu et al., 2025). Furthermore, insulin's central neuromodulatory role in hypothalamic regulation of energy balance through appetite control and metabolic expenditure has been well characterized. Parallel transcriptomic sequencing data revealed congruent pathway enrichment patterns, with DE mRNAs predominantly localized to metabolic and energy transduction pathways,

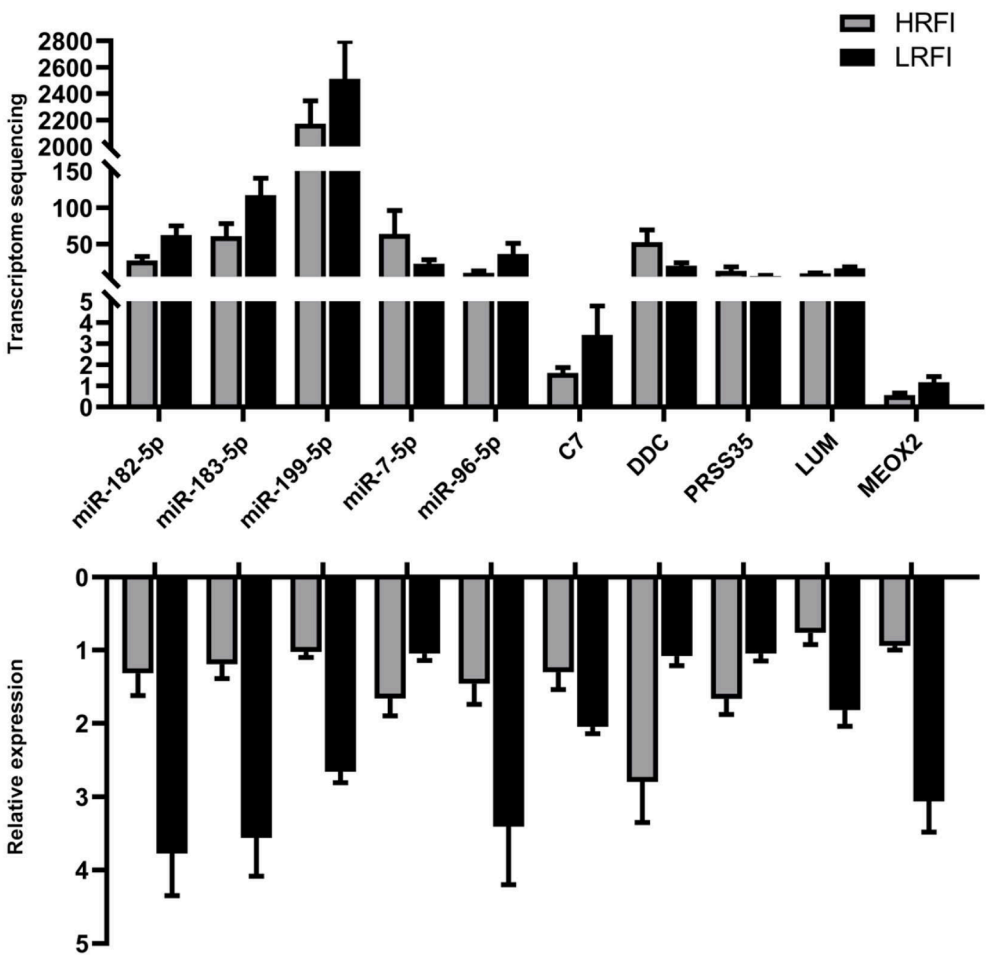

Fig 6. Sequencing results and qPCR verification of 10 genes of interest in hypothalamus samples of meat ducks.

demonstrating consistency with miRNA regulatory network. Therefore, we hypothesize that miRNAs may influence RFI by mediating the expression levels of target genes, thereby regulating the activity of these metabolic pathways.

Through comprehensive WGCNA analysis, we systematically identified 10 candidate hub DE miRNAs: miR-1-3p, miR-10-5p/3p, miR-182-5p/3p, miR-183-5p, miR-263-5p, miR-96-5p, miR-7, and novel-m0108-5p. Expression profiling revealed that all miRNAs except miR-7 and novel-m0108-5p exhibited significant upregulation in LRFI meat ducks, demonstrating a predominant negative correlation with RFI values. To elucidate their regulatory mechanisms, we conducted systematic target prediction and intersected these results with DE mRNAs, ultimately constructing a DE miRNA-mRNA interaction network. Notably, miR-10-5p was computationally predicted to target Protein Phosphatase 1 Regulatory Subunit 17(***PPP1R17)*** and Solute Carrier Family 17 Member 8 (***SLC17A8)***, both showing functional enrichment in neural systems. *PPP1R17*, a regulatory subunit of protein phosphatase 1, modulates intracellular signaling cascades, while *SLC17A8*, a solute carrier protein, facilitates glutamate neurotransmission by regulating neurotransmitter transport, thereby influencing neuronal excitability and synaptic signaling. Though no direct evidence links *PPP1R17* or *SLC17A8* to feeding behavior, we postulate that miR-10-5p may indirectly regulate feed intake through neural signal transduction by targeting these genes. Furthermore, miR-96-5p was identified to target Nuclear Receptor Subfamily 5 Group A Member 1 **(*NR5A1)***, a nuclear receptor critical for steroidogenesis (Morohashi et al., 2020) that governs the expression of gonadotropin-releasing hormone and corticotropin-releasing hormone. Given the established role of these neuropeptides in appetite regulation (Hong et al., 2024), we hypothesize that elevated miR-96-5p expression may enhance feed efficiency through *NR5A1*-mediated modulation of appetite-related hormone synthesis and secretion. These findings collectively suggest that miRNA-mediated regulation of neuroendocrine pathways and metabolic signaling may constitute a novel molecular mechanism underlying RFI variation in meat ducks.

Notably, among these hub miRNAs, miR-182-5p emerged as the most central regulator within the network, exhibiting the highest degree of connectivity and node interactions, underscoring its potential pivotal role in RFI regulation. Previous studies have established miR-182-5p as a critical modulator of systemic glucose homeostasis and hepatic lipid metabolism in mammalian models (Krause et al., 2024), biological processes that are mechanistically aligned with the RFI phenotype under investigation. In our study, we established negative regulatory relationships between miR-182-5p and multiple targets including *DDC,* Uridine Phosphorylase 2 (***UPP2***), *PRSS35*, and *SLCO1C1*. Functional annotations revealed that *UPP2* participates in dCMP catabolism and uridine degradation pathways. Notably, a mechanistic study in rainbow trout demonstrated that *UPP2* signaling suppresses uridine catabolism, thereby ameliorating hepatic lipid accumulation under high-fat dietary conditions (Yu et al., 2025). Intriguingly, *UPP2* has also been identified as a circadian rhythm-regulated gene (Zhao et al., 2024), suggesting potential temporal regulation of feeding behavior in meat ducks. *PRSS35*, a protease implicated in proteolytic cascades, may facilitate dietary protein digestion within the gastrointestinal system. *SLCO1C1*, encoding an organic anion transporter highly expressed in cerebral tissues, governs thyroid hormone uptake and distribution. Given the well-documented role of thyroid hormones in energy metabolism and appetite regulation (Deal et al., 2021), *SLCO1C1* represents a compelling candidate for mediating feed efficiency. *DDC*, a rate-limiting enzyme in

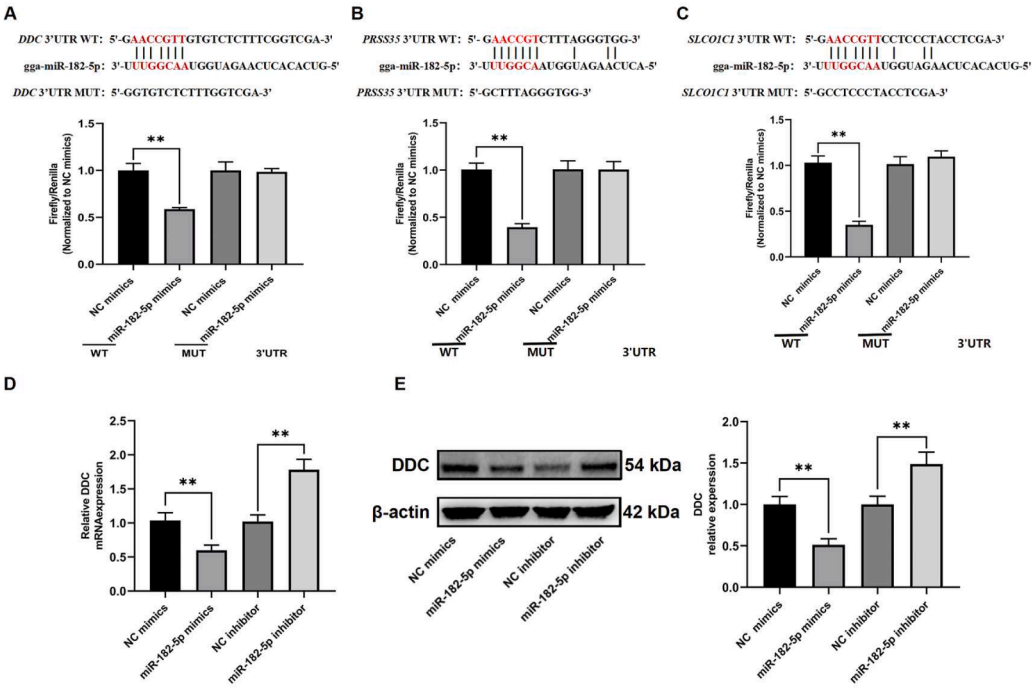

Fig 7. miRNA-mRNA network validation. A, Luciferase reporter assay confirmed that miR-182-5p directly binds to the 3′-UTR of *DDC* mRNA (n = 3). B, Luciferase reporter assay demonstrated the interaction between miR-182-5p and the 3′-UTR of *PRSS35* mRNA (n = 3). C, Luciferase reporter assay demonstrated the interaction between miR-182-5p and the 3′-UTR of *SLCO1C1* mRNA (n = 3). D, RT-qPCR analysis revealed the expression levels of *DDC* mRNA (n = 3). E, Western blot analysis confirmed DDC protein expression (n = 3).

dopamine and serotonin biosynthesis, catalyzes the conversion of L-DOPA to dopamine and 5-hydroxytryptophan to serotonin. The significant upregulation of *DDC* in high-RFI duck hypothalami suggests its involvement in appetite stimulation and feed efficiency modulation via dopaminergic pathways, consistent with the findings on dopamine' s regulatory role in foraging behavior (Goedhoop et al., 2023). Collectively, we propose that miR-182-5p may orchestrate RFI variation through multi-level regulation of lipid metabolism proteolysis, endocrine signaling, and neurotransmission. To validate these interactions, we performed dual-luciferase reporter assays on three representative targets, confirming the presence of functional binding sites and reinforcing the reliability of our predictive framework. Given *DDC*' s critical role in dopamine biosynthesis, We plan to further investigate the regulatory mechanisms of the miR-182-5p-*DDC* pathway in future studies. We substantiated miR-182-5p' s regulatory effect on *DDC* through qPCR and Western blot analyses, providing preliminary mechanistic evidence for its hypothalamic involvement in RFI modulation.

In this study, we constructed a novel miRNA–mRNA network to shed light on the molecular mechanisms by which the hypothalamus regulates RFI. Our study identified a number of negative feedback network that may be critical to RFI regulation, and it is worth noting that, miR-10-5 p*/PPP1R17 / SLC17A8*, miR-96-5p*/UPP2/NR5A1*, miR-182-5p */DDC / PRSS35 / SLCO1C1* is considered to be a key to RFI miRNA-mRNA. While our study advances the understanding of miRNA-mRNA interactions in hypothalamic RFI regulation, limitations must be acknowledged. A primary constraint lies in the absence of in vitro model validation experiments, as current evidence remains confined to target binding verification. Future investigations should prioritize comprehensive mechanistic studies, including tissue-specific knockout models and metabolic flux analyses, to fully elucidate the complex regulatory network governing RFI.

Data availability

The RNA-Seq data presented in this study have been deposited to the National Center for Biotechnology Information under accession number PRJNA891486.

Author Contributions

Hao Bai and Guobin Chang conceived of and designed the study. Dandan Geng, Chunyou Yuan, Xiaofan Li, Chenxiao Wang, Qixin Guo, Yong Jiang, and Zhixiu Wang conducted the tests and engaged in data gathering. Hao Bai and Dandan Geng conducted data analysis and authored the manuscript. Guohong Chen and Guobin Chang amended the manuscript. All authors participated in and endorsed the submitted work.

Declaration of competing interest

This manuscript has not been published or presented elsewhere in part or in entirety and is not under consideration by another journal. The study design was approved by the appropriate ethics review board. We have read and understood your journal's policies, and we believe that neither the manuscript nor the study violates any of these. There are no conflicts of interest to declare.

Acknowledgements

This work was supported by the National Natural Science Foundation of China (31902140), the earmarked fund for CARS (CARS-42), the Jiangsu Provincial Key Research and Development Program (BE2021332) and the "JBGS" Proiect of Seed Industry Revitalization in Jiangsu Province (JBGS[2021]110).

Supplementary materials

Supplementary material associated with this article can be found, in the online version, at doi:10.1016/j.psj.2025.105058.

References

Aderibigbe, A.S., Ajuwon, K.M., Adeola, O., 2022. Dietary phosphorus level regulates appetite through modulation of gut and hypothalamic expression of anorexigenic genes in broiler chickens. Poult. Sci. 101 (2), 101591. https://doi.org/10.1016/j.psj.2021.101591.

Aggrey, S.E., Karnuah, A.B., Sebastian, B., Anthony, N.B., 2010. Genetic properties of feed efficiency parameters in meat-type chickens. Genet. Sel. Evol. 42, 25. https://doi.org/10.1186/1297-9686-42-25.

Bai, H., Guo, Q., Yang, B., Dong, Z., Li, X., Song, Q., Jiang, Y., Wang, Z., Chang, G., Chen, G., 2022a. Effects of residual feed intake divergence on growth performance, carcass traits, meat quality, and blood biochemical parameters in small-sized meat ducks. Poult. Sci. 101 (9), 101990. https://doi.org/10.1016/j.psj.2022.101990.

Bai, H., Shi, L., Guo, Q., Jiang, Y., Li, X., Geng, D., Wang, C., Bi, Y., Wang, Z., Chen, G., Xue, F., Chang, G., 2022b. Metagenomic insights into the relationship between gut microbiota and residual feed intake of small-sized meat ducks. Front. Microbiol. 13, 1075610. https://doi.org/10.3389/fmicb.2022.1075610.

Cantalapiedra-Hijar, G., Abo-Ismail, M., Carstens, G.E., Guan, L.L., Hegarty, R., Kenny, D. A., McGee, M., Plastow, G., Relling, A., Ortigues-Marty, I., 2018. Review: Biological determinants of between-animal variation in feed efficiency of growing beef cattle. Animal. 12 (s2), s321–s335. https://doi.org/10.1017/S1751731118001489.

Chen, S., Zhou, Y., Chen, Y., Gu, J., 2018. fastp: an ultra-fast all-in-one FASTQ preprocessor. Bioinformatics. 34 (17), i884–i890. https://doi.org/10.1093/bioinformatics/bty560.

Crews, D.J., 2005. Genetics of efficient feed utilization and national cattle evaluation: a review. Genet. Mol. Res. 4 (2), 152–165.

Deal, C.K., Volkoff, H., 2021. Response of the thyroid axis and appetite-regulating peptides to fasting and overfeeding in goldfish (Carassius auratus). Mol. Cell. Endocrinol. 528, 111229. https://doi.org/10.1016/j.mce.2021.111229.

De Oliveira, P.S.N., Coutinho, L.L., Tizioto, P.C., Cesar, A.S.M., de Oliveira, G.B., Diniz, W.J.d.S., De Lima, A.O., Reecy, J.M., Mourão, G.B., Zerlotini, A., Regitano, L. C.A., 2018. An integrative transcriptome analysis indicates regulatory mRNA-miRNA networks for residual feed intake in Nelore cattle. Sci. Rep. 8 (1), 17072. https://doi.org/10.1038/s41598-018-35315-5.

Devis, P., Yogi, P.M., Francesca, G., Mauro, G., Saveria, C.L., Claudio, T., 2020. Weighted miRNA co-expression networks analysis identifies circulating miRNA predicting overall survival in hepatocellular carcinoma patients. Sci. Rep. 10 (1), 18967. https://doi.org/10.1038/s41598-020-75945-2.

Goedhoop, J., Arbab, T., Willuhn, I., 2023. Anticipation of Appetitive Operant Action Induces Sustained Dopamine Release in the Nucleus Accumbens. J. Neurosci. 43, 3922–3932. https://doi.org/10.1523/jneurosci.1527-22.2023.

He, Y., Zhang, C., Luo, Y., Chen, J., Yang, M., Li, L., Gu, H.F., Yang, G., Zhang, X., 2021. Hypothalamic BMP9 suppresses glucose production by central PI3K/Akt/mTOR pathway. J. Endocrinol. 248 (2), 221–235. https://doi.org/10.1530/JOE-19-0591.

Hong, S.H., M, K., 2024. Choi. Gut hormones and appetite regulation. Curr. Opin. Endocrinol. Diabetes Obes. 31 (3), 115–121. https://doi.org/10.1097/MED.0000000000000859.

Jing, L., Hou, Y., Wu, H., Miao, Y., Li, X., Cao, J., Brameld, J.M., Parr, T., Zhao, S., 2015. Transcriptome analysis of mRNA and miRNA in skeletal muscle indicates an important network for differential Residual Feed Intake in pigs. Sci. Rep. 5, 11953. https://doi.org/10.1038/srep11953.

Koch, R.M., Swiger, L.A., Chambers, D., Gregory, K.E., 1963. Efficiency of Feed Use in Beef Cattle. J. Anim. Sci. 22 (2), 486–494. https://doi.org/10.2527/jas1963.222486x.

Krause, C., Britsemmer, J.H., Bernecker, M., Molenaar, A., Taege, N., Lopez-Alcantara, N., Geißler, C., Kaehler, M., Iben, K., Judycka, A., Wagner, J., Wolter, S., Mann, O., Pfluger, P., Cascorbi, I., Lehnert, H., Stemmer, K., Schriever, S.C., Kirchner, H., 2024. Liver microRNA transcriptome reveals miR-182 as link between type 2 diabetes and fatty liver disease in obesity. Elife 12, RP92075. https://doi.org/10.7554/eLife.92075.

Li, X., Yang, B., Dong, Z., Geng, D., Wang, C., Guo, Q., Jiang, Y., Chen, G., Chang, G., Bai, H., 2023. Growth performance, carcass traits, meat quality, and blood variables of small-sized meat ducks with different feed efficiency phenotypes. Poult. Sci. 102 (8), 102818. https://doi.org/10.1016/j.psj.2023.102818.

Listrat, A., Lebret, B., Louveau, I., Astruc, T., Bonnet, M., Lefaucheur, L., Picard, B., Bugeon, J., 2016. How Muscle Structure and Composition Influence Meat and Flesh Quality. Sci. World J. 2016, 3182746. https://doi.org/10.1155/2016/3182746.

Liu, J., Liu, R., Wang, J., Zhang, Y., Xing, S., Zheng, M., Cui, H., Li, Q., Li, P., Cui, X., Li, W., Zhao, G., Wen, J., 2018. Exploring Genomic Variants Related to Residual Feed Intake in Local and Commercial Chickens by Whole Genomic Resequencing. Genes. (Basel) 9 (2), 57. https://doi.org/10.3390/genes9020057.

Liu, R., Liu, J., Zhao, G., Li, W., Zheng, M., Wang, J., Li, Q., Cui, H., Wen, J., 2019. Relevance of the intestinal health-related pathways to broiler residual feed intake revealed by duodenal transcriptome profiling. Poult. Sci. 98 (3), 1102–1110. https://doi.org/10.3382/ps/pey506.

Luo, C., Sun, L., Ma, J., Wang, J., Qu, H., Shu, D., 2015. Association of single nucleotide polymorphisms in the microRNA miR-1596 locus with residual feed intake in chickens. Anim. Genet. 46 (3), 265–271. https://doi.org/10.1111/age.12284.

Livak, K.J., Schmittgen, T.D., 2001. Analysis of relative gene expression data using real-time quantitative PCR and the 2(-Delta Delta C(T)) Method. Methods 25 (4), 402–408. https://doi.org/10.1006/meth.2001.1262.

Mokshata, G., Tanmay, M., 2021. Heat stress and thermoregulatory responses of goats: a review. Biol. Rhythm. Res. 52.

Morohashi, K.I., Inoue, M., Baba, T., 2020. Coordination of Multiple Cellular Processes by NR5A1/Nr5a1. Endocrinol. Metab (Seoul). 35 (4), 756–764. https://doi.org/10.3803/EnM.2020.402.

Mota, L.F.M., Bonafé, C.M., Alexandre, P.A., Santana, M.H., Novais, F.J., Toriyama, E., Pires, A.V., da Luz Silva, S., Leme, P.R., Ferraz, J.B.S., Fukumasu, H., 2017. Circulating leptin and its muscle gene expression in Nellore cattle with divergent feed efficiency. J. Anim. Sci. Biotechnol. 8, 71. https://doi.org/10.1186/s40104-017-0203-3.

Nouchi, Y., Munetsuna, E., Yamada, H., Yamazaki, M., Ando, Y., Mizuno, G., Ikeya, M., Kageyama, I., Wakasugi, T., Teshigawara, A., Hattori, Y., Tsuboi, Y., Ishikawa, H., Suzuki, K., 2023. Maternal High-Fructose Corn Syrup Intake Impairs Corticosterone Clearance by Reducing Renal 11β-Hsd2 Activity via miR-27a-Mediated Mechanism in Rat Offspring. Nutrients 15 (9), 2122. https://doi.org/10.3390/nu15092122.

Núria, S.B., Laia, R., Francesc, P., 2022. Improved biomarker discovery through a plot twist in transcriptomic data analysis. BMC Bio 20 (1), 208. https://doi.org/10.1186/s12915-022-01398-w.

Tran, P.V., Chowdhury, V.S., Do, P.H., Bahry, M.A., Yang, H., Furuse, M., 2016. L-Ornithine is a potential acute satiety signal in the brain of neonatal chicks. Physiol. Behav. 155, 141–148. https://doi.org/10.1016/j.physbeh.2015.12.007.

Wu, L., Zhuang, Z., Jia, W., Li, Y., Lu, Y., Xu, M., Bai, H., Wang, Z., Chang, G., Jiang, Y., 2025. Exploring the molecular basis of efficient feed utilization in low residual feed intake slow-growing ducks based on breast muscle transcriptome. Poult.. Sci. 104 (1), 104613. https://doi.org/10.1016/j.psj.2024.104613.

Yang, Y., Sang, Z., Xu, C., Dai, W., Zou, C., 2019. Identification of maize flowering gene co-expression modules by WGCNA. Acta Agronomica Sinica 45, 161. https://doi.org/10.3724/SP.J.1006.2019.83053.

Yousefvand, S., Hamidi, F., 2022. Role of Lateral Hypothalamus Area in the Central Regulation of Feeding. Int. J. Pept. Res. Ther. 28, 83. https://doi.org/10.1007/s10989-022-10391-4.

Yu, H.X., Mo, H.L., An, X.R., Yao, M.G., Gao, J.W., Yu, J.J., Xiong, D.G., Liu, H.X., Li, Y., Wang, L.X., 2025. Autocrine/paracrine fibroblast growth factor 1 (FGF1) enhances systemic lipid metabolism in rainbow trout fed with a high-fat diet by elevating uridine levels through the AMPK signaling pathway and activating the upp2 promoter via irf1. Aquaculture 59 (2), 741885. https://doi.org/10.1016/j.aquaculture.2024.741885.

Yuan, R., Cai, B., Ma, M., Zhao, C., Xian, Y., Nie, Q., Zhang, X., Zhang, D., 2024. LncEDCH1 g.1703613 T>C regulates chicken carcass traits by targeting miR-196-2-3p. Poult. Sci. 103 (3), 103412. https://doi.org/10.1016/j.psj.2023.103412.

Zeng, T., Chen, L., Du, X., Lai, S.J., Huang, S.P., Liu, Y.L., Lu, L.Z., 2016. Association analysis between feed efficiency studies and expression of hypothalamic neuropeptide genes in laying ducks. Anim. Genet. 47, 606–609. https://doi.org/10.1111/age.12457.

Zhai, B., Li, H., Li, S., Gu, J., Zhang, H., Zhang, Y., Li, H., Tian, Y., Li, G., Wang, Y., 2023. Transcriptome analysis reveals FABP5 as a key player in the development of chicken abdominal fat, regulated by miR-122-5p targeting. BMC. Genomics. 24 (1), 386. https://doi.org/10.1186/s12864-023-09476-1.

Zhang, S.P., Lu, Y.P., Li, Y.Z., Liu, Y.L., Yao, Q., Kang, Q., Chen, S.H., Liu, Y.L., Xiong, Y. X., Chen, D.F., Zhang, X., Tang, N., Li, Z.Q., 2024. Brain-derived neurotrophic factor (BDNF) activates PI3K-AKT-mTOR signaling via hypothalamic TrkB receptors to reduce feeding in Siberian sturgeon (Acipenser baerii). Aquaculture 579, 740196. https://doi.org/10.1016/j.aquaculture.2023.740196.

Zhang, Y., Guo, Z.B., Xie, M., Zhang, Z., Hou, S., 2017. Genetic parameters for residual feed intake in a random population of Pekin duck. Asian-Australas J. Anim. Sci. 30 (2), 167–170. https://doi.org/10.5713/ajas.15.0577.

Zhao, H.C., Han, G.H., Jiang, Z., Gao, D.K., Zhang, H.S., Yang, L.D., Ma, T.T., Gao, L., Wang, A.H., Chao, H., Li, Q., Jin, Y.P., Chen, H.T., 2024. Identification of BMAL1-Regulated circadian genes in mouse liver and their potential association with hepatocellular carcinoma: Gys2 and Upp2 as promising candidates. Biochem. Biophys. Res. Commun. 696, 149422. https://doi.org/10.1016/j.bbrc.2023.149422.